

**Rotational and Vibrational Spectroscopy of a Weakly Bound Hexafluoroisopropanol···Nitrogen Complex:  $^{14}\text{N}$  Hyperfine Splittings, Molecular Geometry, and Experimental Benchmarks**

Shauna E. Beresnak,<sup>a</sup> Sönke Oswald,<sup>a,b</sup> Bowei Wu,<sup>a</sup> Nathan A. Seifert,<sup>c</sup> Martin A. Suhm,<sup>b</sup> Wolfgang Jäger<sup>a</sup> and Yunjie Xu<sup>\*a</sup>

<sup>a</sup> Department of Chemistry, University of Alberta, 11227 Saskatchewan Drive, Edmonton, Canada

<sup>b</sup> Institut für Physikalische Chemie, Georg-August-Universität Göttingen, Tammannstraße 6, 37077, Göttingen, Germany

<sup>c</sup> Chemistry and Chemical & Biomedical Engineering Department, University of New Haven, 300 Boston Post Rd, West Haven, CT, 06516, USA.

\* Corresponding author

Contents

<b>Table S1.</b> Spectroscopic properties of the most stable HFIP and HFIP···N <sub>2</sub> conformers at the B3LYP-D3(BJ)/def2-QZVP level of theory .....	S2
<b>Table S2.</b> Cartesian coordinates of the eleven most stable HFIP···N <sub>2</sub> conformers .....	S2-S4
<b>Figure S1.</b> CP-FTMW spectrum with previously identified species .....	S5
<b>Table S3-S4.</b> Assigned rotational transition frequencies of H <sub>2</sub> NH .....	S6-S8
<b>Figure S2-S4.</b> Relative deviation of the predicted rotational constants from the experimental rotational constant for HFIP and H <sub>2</sub> NH at multiple levels of theory .....	S9-S10
<b>Table S5.</b> Theoretical rotational constants, $\omega_{\text{OH}}$ , $\Delta\omega_{\text{OH}}$ , and $\omega_1$ at multiple levels of theory .	S10-S11
<b>References</b> .....	S11

**Table S1.** Spectroscopic properties of the most stable HFIP and HFIP $\cdots$ N<sub>2</sub> conformers at the B3LYP-D3(BJ)/def2-QZVP level of theory.

Parameter	H <sub>t</sub>	H <sub>t</sub> N <sub>H</sub>	H <sub>t</sub> N <sub>C</sub>	H <sub>t</sub> N <sub>O</sub>	H <sub>t</sub> N <sub>F</sub>	H <sub>t</sub> N <sub>F<sup>-</sup></sub>	H <sub>g</sub>	H <sub>g</sub> N <sub>H</sub>	H <sub>g</sub> N <sub>C</sub>	H <sub>g</sub> N <sub>O</sub>	H <sub>g</sub> N <sub>F</sub>	H <sub>g</sub> N <sub>F<sup>-</sup></sub>	
$\Delta E_e$ /kJ mol <sup>-1</sup> <sup>a</sup>	(0.0)	(0.0)	4.6	4.8	7.4	8.4	4.7	5.2	9.6	11.8	12.2	13.1	13.1
$\Delta E_0$ /kJ mol <sup>-1</sup> <sup>a</sup>	(0.0)	(0.0)	3.3	3.5	5.5	6.2	4.1	4.5	7.6	9.2	9.6	10.3	10.3
A <sub>e</sub> /MHz <sup>b</sup>	2089.8	958.2	947.7	1078.3	979.7	1825.4	2093.2	1224.7	956.2	1375.2	987.8	1781.6	1585.9
B <sub>e</sub> /MHz <sup>b</sup>	1042.2	743.0	766.8	643.2	830.8	474.5	1043.8	544.9	755.0	575.0	816.5	481.1	505.3
C <sub>e</sub> /MHz <sup>b</sup>	922.9	535.7	551.3	502.4	572.1	444.8	923.8	442.4	550.2	480.3	563.0	448.0	451.7
$\mu_a$   /Debye <sup>c</sup>	0.0	0.8	0.1	0.5	0.6	0.2	1.1	2.7	0.8	0.4	2.3	1.7	0.0
$\mu_b$   /Debye <sup>c</sup>	0.6	0.0 <sup>d</sup>	0.0 <sup>d</sup>	0.3	0.0 <sup>d</sup>	0.6	1.3	0.6	1.2	1.4	0.6	1.2	2.1
$\mu_c$   /Debye <sup>c</sup>	0.1	0.4	0.5	0.3	0.2	0.0	1.9	1.4	2.1	2.0	0.8	1.5	1.4
$\chi_{aa}(N_i)$ /MHz <sup>e</sup>	-	-3.040	-3.665	-3.210	2.790	3.016	-	-5.431	-2.792	2.947	2.500	2.979	2.964
$\chi_{bb} - \chi_{cc}(N_i)$ /MHz <sup>e</sup>	-	2.733	2.282	2.762	8.853	5.943	-	0.133	3.012	2.632	2.501	8.486	-8.223
$\chi_{aa}(N_o)$ /MHz <sup>e</sup>	-	-3.222	-3.752	-3.262	2.812	3.011	-	-5.812	-2.856	2.942	2.467	2.977	2.979
$\chi_{bb} - \chi_{cc}(N_o)$ /MHz <sup>e</sup>	-	2.916	2.378	2.858	8.883	5.925	-	0.102	3.130	2.631	2.506	8.476	-8.247
$\omega_{OH}$ /cm <sup>-1</sup> <sup>f</sup>	3789	3753	3790	3789	3788	3789	3827	3797	3829	3829	3827	3826	3827

<sup>a</sup>  $\Delta E_e$  and  $\Delta E_0$  are the relative raw and harmonic vibrational zero-point energy (ZPE) corrected energy in kJ mol<sup>-1</sup>, respectively. They are relative to H<sub>t</sub> and H<sub>t</sub>N<sub>H</sub>, for the monomer and complex conformers, respectively. <sup>b</sup> Equilibrium rotational constants. <sup>c</sup> Magnitudes of the a-, b- and c-type electric dipole moment components. <sup>d</sup> This dipole moment component is 0 due to symmetry reasons. <sup>e</sup> Nuclear quadrupole coupling constants with N<sub>i</sub> and N<sub>o</sub> referring to the inner (closer to HFIP) and outer nitrogen, respectively. <sup>f</sup> Harmonic OH stretching wavenumber.

**Table S2.** Cartesian coordinates (in Å) of the eleven most stable HFIP $\cdots$ N<sub>2</sub> conformers obtained at the B3LYP-D3(BJ)/def2-QZVP geometry optimizations with convergence set to 'verytight' and integration grid to 'SuperFine'.

H <sub>t</sub> N <sub>H</sub>	a	b	c	H <sub>t</sub> N <sub>C</sub>	a	b	c
C	0.71978	1.29141	0.02707	C	-0.47634	1.29181	0.12232
C	0.65984	0.00000	-0.81107	C	-0.45328	-0.00001	-0.71559
H	1.54351	0.00000	-1.44798	H	0.48223	0.00001	-1.27056
C	0.71978	-1.29141	0.02707	C	-0.47629	-1.29182	0.12232
F	0.75848	2.35166	-0.79129	F	-0.33836	2.35016	-0.68753
F	-0.36956	1.42154	0.80814	F	-1.64694	1.42868	0.77422
F	1.80215	1.34154	0.81345	F	0.50971	1.33726	1.02658
F	1.80215	-1.34154	0.81345	F	0.50977	-1.33724	1.02657
F	0.75848	-2.35166	-0.79129	F	-0.33828	-2.35017	-0.68753
F	-0.36956	-1.42154	0.80814	F	-1.64688	-1.42873	0.77423
O	-0.45946	0.00000	-1.63975	O	-1.49762	-0.00003	-1.64233
H	-1.26633	0.00000	-1.10927	H	-2.34216	-0.00004	-1.17806
N	-3.16970	0.00000	-0.08008	N	3.99591	0.00004	-0.00610
N	-4.06992	0.00000	0.53277	N	3.05709	0.00006	-0.55899

H <sub>t</sub> N <sub>O</sub>	a	b	c	H <sub>g</sub> N <sub>H</sub>	a	b	c
C	-1.39319	-0.85249	-0.11856	C	-1.61780	-0.74936	-0.10529
C	0.02057	-0.26384	0.03903	C	-0.15155	-0.31556	-0.25231
H	0.61686	-0.63764	-0.79099	H	0.11392	-0.48999	-1.29902
C	0.07261	1.27354	-0.02932	C	0.07927	1.18710	0.00230
F	-1.31624	-2.18956	-0.16057	F	-1.74567	-2.02468	-0.50235
F	-2.17714	-0.52362	0.92609	F	-2.05313	-0.66321	1.15332
F	-1.99828	-0.44086	-1.23860	F	-2.41942	0.00109	-0.87883
F	-0.45968	1.75442	-1.15857	F	-0.49409	1.94521	-0.94234
F	1.34915	1.67838	0.02756	F	1.41021	1.42299	-0.04522
F	-0.57613	1.83101	1.01078	F	-0.36074	1.59345	1.19418
O	0.61208	-0.72096	1.21848	O	0.59141	-1.09206	0.63593
H	0.10335	-0.41199	1.97645	H	1.52529	-1.04292	0.40715
N	3.24179	-1.04366	-0.59265	N	3.63448	-0.97362	-0.07668
N	4.14685	-1.05439	0.01378	N	4.70326	-0.85973	-0.25226
H <sub>t</sub> N <sub>F</sub>	a	b	c	H <sub>t</sub> N <sub>F'</sub>	a	b	c
C	0.47597	1.29270	0.15979	C	0.56022	0.27772	-0.24337
C	1.31376	0.00006	0.16826	C	-0.90938	0.66797	-0.48853
H	1.88634	0.00010	1.09447	H	-1.04413	0.73280	-1.56712
C	0.47610	-1.29266	0.15981	C	-1.92792	-0.36528	0.02916
F	1.28923	2.35052	0.27746	F	1.36283	1.18357	-0.81886
F	-0.20060	1.42603	-0.99674	F	0.84611	0.25911	1.07211
F	-0.40589	1.33914	1.16519	F	0.86471	-0.92158	-0.75249
F	-0.40580	-1.33915	1.16518	F	-1.71437	-1.58902	-0.46782
F	1.28945	-2.35040	0.27755	F	-3.16345	0.01231	-0.32523
F	-0.20042	-1.42610	-0.99673	F	-1.89706	-0.44703	1.37276
O	2.22450	0.00009	-0.88916	O	-1.17649	1.92952	0.04517
H	1.74788	0.00005	-1.72693	H	-1.06719	1.90592	1.00249
N	-3.21301	-0.00031	-0.82167	N	4.25625	-0.65290	-0.25410
N	-3.38442	0.00006	0.25467	N	4.21248	-0.19971	0.73618
H <sub>g</sub> N <sub>C</sub>	a	b	c	H <sub>g</sub> N <sub>O</sub>	a	b	c
C	-0.16314	1.32588	0.13528	C	-0.32283	1.02909	-0.09691
C	-0.44822	0.07641	-0.71027	C	0.36668	-0.23944	-0.62095
H	0.48485	-0.16328	-1.22537	H	0.55190	-0.07009	-1.68546
C	-0.81201	-1.16746	0.12219	C	1.74262	-0.50931	0.01766
F	0.30955	2.30055	-0.65583	F	-1.42317	1.26962	-0.82672
F	-1.25221	1.78679	0.75316	F	-0.69071	0.92047	1.18062
F	0.76982	1.06772	1.06719	F	0.48661	2.09337	-0.21379
F	0.23144	-1.61059	0.83601	F	2.64897	0.40294	-0.35455
F	-1.16391	-2.15439	-0.73409	F	2.17634	-1.71390	-0.42046
F	-1.83691	-0.96828	0.95215	F	1.70717	-0.55245	1.34998
O	-1.48582	0.41225	-1.58517	O	-0.51191	-1.29936	-0.38322
H	-1.58206	-0.27783	-2.24715	H	-0.19882	-2.08629	-0.83773

N	3.93120	-0.65470	0.04048	N	-3.85552	-0.61884	0.56119
N	3.05651	-0.55796	-0.60193	N	-3.77112	-1.26535	-0.31202
H <sub>g</sub> N <sub>F</sub>	a	b	c	H <sub>g</sub> N <sub>F'</sub>	a	b	c
C	0.23361	1.32887	0.16810	C	-0.55618	-0.36547	-0.19796
C	1.29937	0.22311	0.15596	C	0.92348	-0.70652	-0.42698
H	1.83850	0.30736	1.10410	H	1.04894	-0.81441	-1.50834
C	0.71682	-1.20276	0.11922	C	1.89300	0.40900	0.00845
F	0.82654	2.51671	0.35584	F	-1.32307	-1.31798	-0.74886
F	-0.45755	1.38690	-0.97185	F	-0.86886	-0.28096	1.09633
F	-0.63394	1.13998	1.17589	F	-0.86954	0.80213	-0.78297
F	0.08943	-1.51193	1.25953	F	1.79303	1.48740	-0.77824
F	1.74677	-2.06917	-0.02571	F	3.15491	-0.06565	-0.11278
F	-0.12471	-1.40409	-0.89622	F	1.72550	0.79125	1.27486
O	2.11193	0.46147	-0.95520	O	1.17483	-1.89043	0.27080
H	2.86891	-0.13063	-0.93225	H	2.05501	-2.21027	0.05376
N	-3.45352	-0.14490	-0.68436	N	-4.16159	0.60781	0.73186
N	-3.18818	-0.77344	0.16555	N	-4.24119	0.41599	-0.33811
H <sub>g</sub> N <sub>F'</sub>	a	b	c				
.							
C	-1.80874	0.53299	-0.00926				
C	-1.02084	-0.74278	-0.34204				
H	-1.21807	-0.95827	-1.39626				
C	0.50604	-0.58125	-0.21563				
F	-3.10413	0.34454	-0.30111				
F	-1.71957	0.86884	1.27883				
F	-1.36897	1.56671	-0.74499				
F	0.99778	0.23195	-1.15904				
F	1.07028	-1.79755	-0.39400				
F	0.89276	-0.12721	0.97764				
O	-1.49189	-1.74074	0.51467				
H	-1.11745	-2.58787	0.25715				
N	4.16491	1.25434	0.33705				
N	4.08319	0.19198	0.10781				

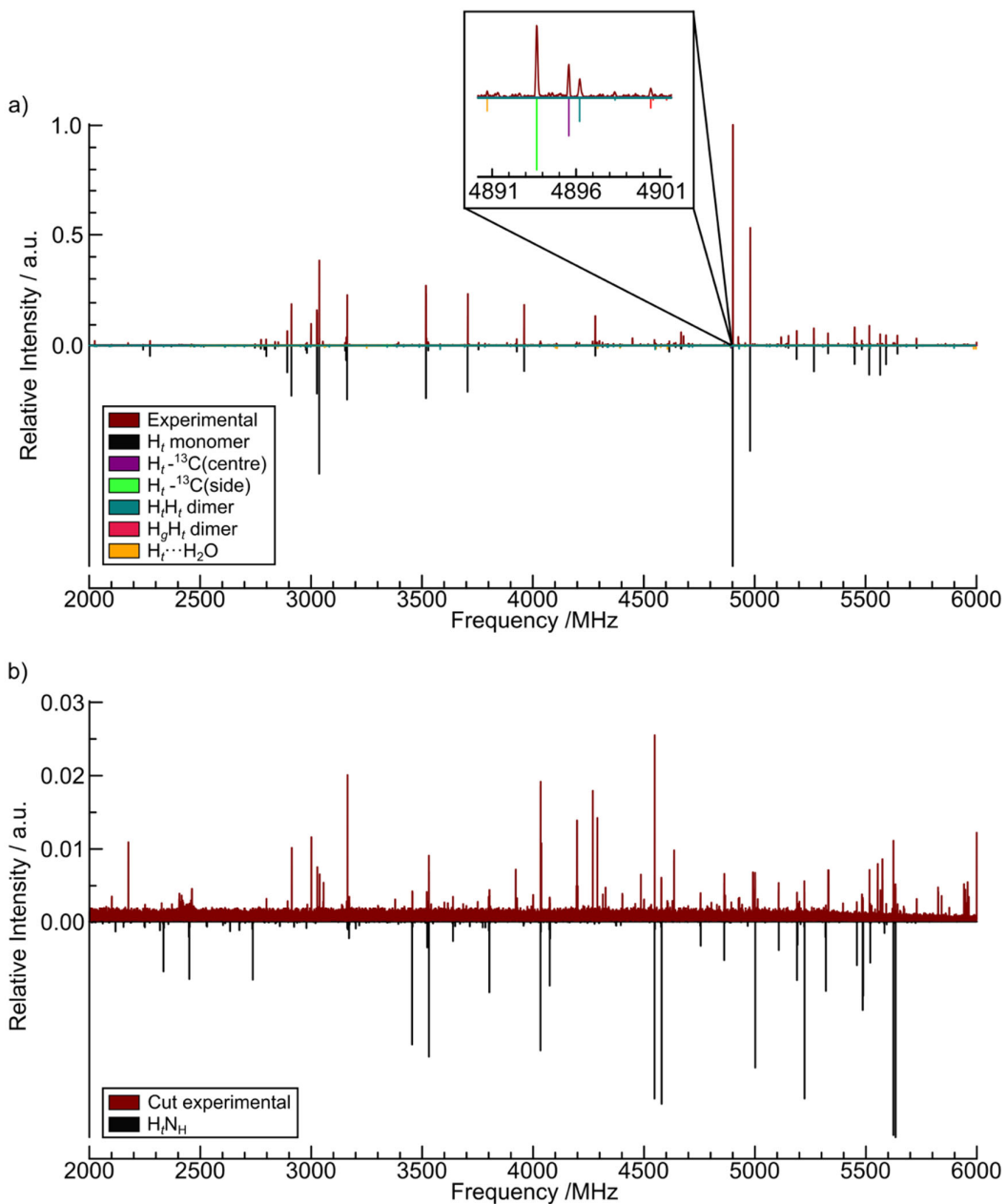


**Figure S1.** a) The CP-FTMW spectrum (top), recorded with HFIP and  $\text{N}_2$  in helium carrier gas, is dominated by strong transitions from previously reported species. These include the *trans*-HFIP monomer and its two  $^{13}\text{C}$  isotopologues,<sup>i</sup> the achiral  $\text{H}_t\text{H}_t$  and chiral  $\text{H}_g\text{H}_t$  HFIP dimers,<sup>ii</sup> and the most stable conformer of  $\text{HFIP}\cdots\text{H}_2\text{O}$ .<sup>iii,iv</sup> The simulated spectrum for these species, based on their known experimental spectroscopic constants and a rotational temperature of 1 K, as well as the theoretical permanent dipole components, are shown in the bottom trace. The insert highlights a small section of the experimental spectrum, alongside the corresponding simulated spectra of multiple species. b) The CP-FTMW spectrum (top) after removing all the transitions of the known species indicated in a). The simulated spectrum (bottom) of  $\text{H}_2\text{N-H}$  based on the experimental spectroscopic constants and a rotational temperature of 1 K, as well as the theoretical permanent dipole components is shown in the bottom trace.

**Table S3.** Experimentally assigned hypothetical unsplit central transition frequencies of H<sub>t</sub>NH.

J'	Ka'	Kc'	J''	Ka''	Kc''	RSD <sup>a</sup>	v <sup>b</sup> /MHz	Δv <sup>c</sup> /MHz
3	1	3	-	2	1	2	3455.5582	-0.0002
2	2	0	-	1	1	0	3522.8481	0.0050
3	0	3	-	2	0	2	3530.2713	-0.0001
2	2	1	-	1	1	1	3638.6571	0.0000
3	2	2	-	2	2	1	3802.7200	-0.0052
3	2	1	-	2	2	0	4075.2456	-0.0003
4	0	4	-	3	0	3	4578.4565	-0.0001
3	1	2	-	2	0	2	4754.7986	0.0048
3	2	1	-	2	1	1	4861.8029	-0.0051
4	2	3	-	3	2	2	5000.9404	-0.0002
3	2	2	-	2	1	2	5107.2492	-0.0050
4	1	3	-	3	1	2	5223.1466	0.0022
4	2	2	-	3	2	1	5486.7268	-0.0053
5	1	5	-	4	1	4	5624.5241	0.0018
5	1	4	-	4	1	3	6297.6518	0.0013
4	1	3	-	3	0	3	6447.6655	-0.0013
4	2	3	-	3	1	3	6652.6346	-0.0019
6	0	6	-	5	0	5	6696.5727	-0.0042
5	2	3	-	4	2	2	6811.0406	0.0007
4	3	2	-	3	2	2	6907.2423	0.0011
6	1	5	-	5	1	4	7328.7583	-0.0005
6	3	4	-	5	3	3	7686.0070	0.0014
7	1	7	-	6	1	6	7761.0908	-0.0006
7	0	7	-	6	0	6	7761.7640	0.0018
6	4	3	-	5	4	2	7846.3668	-0.0014
6	2	4	-	5	2	3	8007.4720	-0.0002
6	4	2	-	5	4	1	8008.8896	0.0021
5	3	2	-	4	2	2	8009.8774	0.0002
5	1	4	-	4	0	4	8166.8625	0.0019
6	3	3	-	5	3	2	8245.1805	-0.0015
7	2	6	-	6	2	5	8346.3349	-0.0011
7	1	6	-	6	1	5	8370.5503	0.0010
8	1	8	-	7	1	7	8827.5562	0.0002
8	0	8	-	7	0	7	8827.7180	-0.0012
7	3	5	-	6	3	4	8856.4190	0.0002
7	2	5	-	6	2	4	9075.2669	-0.0016
8	3	6	-	7	3	5	9979.8760	0.0008
8	4	5	-	7	4	4	10382.7507	-0.0004
10	1	10	-	9	1	9	10960.0021	0.0002
10	0	10	-	9	0	9	10960.0106	0.0001

<sup>a</sup> The hypothetical unsplit central frequencies extracted from the cavity-based measurements were given a relative uncertainty of 1, whereas a value of 2 was used for those obtained from the broadband measurements.

<sup>b</sup> Experimental transition frequency

<sup>c</sup> Experimental transition frequency – theoretical transition frequency

**Table S4.** Experimentally assigned  $^{14}\text{N}$  hyperfine components of  $\text{H}_t\text{N}_\text{H}$ .

J'	Ka'	Kc'	$I_{\text{N}}'$ <sup>a</sup>	F' <sup>a</sup>		J''	Ka''	Kc''	$I_{\text{N}}''$ <sup>a</sup>	F'' <sup>a</sup>	$\nu$ <sup>b</sup> /MHz	$\Delta\nu$ <sup>c</sup> /MHz
4	1	3	2	2	-	3	1	2	2	1	5222.8621	0.0033
4	1	3	2	3	-	3	1	2	2	2	5222.9621	0.0023
4	1	3	0	4	-	3	1	2	0	3	5222.9762	0.0012
4	1	3	1	4	-	3	1	2	1	3	5223.0245	0.0022
4	1	3	2	6	-	3	1	2	2	5	5223.0963	0.0016
4	1	3	1	5	-	3	1	2	1	4	5223.1693	0.0013
4	1	3	1	3	-	3	1	2	1	2	5223.2865	0.0037
4	1	3	2	5	-	3	1	2	2	4	5223.3135	0.0016
4	1	3	2	4	-	3	1	2	2	3	5223.3441	0.0027
5	1	4	2	3	-	4	1	3	2	2	6297.4110	0.0003
5	1	4	0	5	-	4	1	3	0	4	6297.4863	0.0004
5	1	4	1	5	-	4	1	3	1	4	6297.5087	0.0036
5	1	4	2	7	-	4	1	3	2	6	6297.5635	0.0002
5	1	4	2	4	-	4	1	3	2	3	6297.5764	0.0024
5	1	4	1	6	-	4	1	3	1	5	6297.6952	0.0018
5	1	4	1	4	-	4	1	3	1	3	6297.7721	0.0028
5	1	4	2	6	-	4	1	3	2	5	6297.8059	0.0013
5	1	4	2	5	-	4	1	3	2	4	6297.9172	0.0011
4	3	2	1	5	-	3	2	2	1	4	6907.2833	0.0004
4	3	2	1	3	-	3	2	2	1	2	6907.3238	0.0024
4	3	2	1	3	-	3	2	2	1	3	6907.3241	0.0021
4	3	2	2	5	-	3	2	2	2	4	6907.3464	-0.0010
4	3	2	2	5	-	3	2	2	2	5	6907.3466	-0.0012
4	3	2	2	4	-	3	2	2	2	3	6907.4637	-0.0005
4	3	2	2	4	-	3	2	2	2	4	6907.4634	-0.0001
6	1	5	2	4	-	5	1	4	2	3	7328.6236	-0.0008
6	1	5	0	6	-	5	1	4	0	5	7328.6616	-0.0008
6	1	5	2	8	-	5	1	4	2	7	7328.7004	-0.0006
6	1	5	2	5	-	5	1	4	2	4	7328.7329	-0.0003
6	1	5	1	7	-	5	1	4	1	6	7328.7892	0.0000
6	1	5	2	7	-	5	1	4	2	6	7328.8487	-0.0010
6	1	5	2	6	-	5	1	4	2	5	7328.9290	0.0000
6	3	4	2	6	-	5	3	3	2	5	7685.7752	0.0019
6	3	4	2	8	-	5	3	3	2	7	7686.1034	0.0016
6	3	4	1	6	-	5	3	3	1	5	7686.1215	0.0020
6	3	4	0	6	-	5	3	3	0	5	7686.1234	0.0000
6	3	4	2	4	-	5	3	3	2	3	7686.1433	0.0012
6	4	3	2	7	-	5	4	2	2	6	7846.0972	0.0029
6	4	3	1	5	-	5	4	2	1	4	7846.1541	0.0014

6	4	3	1	7	-	5	4	2	1	6	7846.2438	0.0031
6	4	3	2	5	-	5	4	2	2	4	7846.3627	0.0016
6	4	3	1	6	-	5	4	2	1	5	7846.6917	0.0009
6	4	3	0	6	-	5	4	2	0	5	7846.7080	0.0032
6	4	3	2	4	-	5	4	2	2	3	7846.7954	0.0034
6	2	4	2	8	-	5	2	3	2	7	8007.4197	0.0003
6	2	4	2	5	-	5	2	3	2	4	8007.4197	0.0002
6	2	4	1	7	-	5	2	3	1	6	8007.4988	-0.0006
6	2	4	1	5	-	5	2	3	1	4	8007.5513	0.0008
6	2	4	2	6	-	5	2	3	2	5	8007.6430	-0.0007
6	4	2	2	7	-	5	4	1	2	6	8008.5352	0.0005
6	4	2	1	5	-	5	4	1	1	4	8008.6083	0.0011
6	4	2	1	7	-	5	4	1	1	6	8008.7209	0.0006
6	4	2	2	5	-	5	4	1	2	4	8008.8675	0.0003
6	4	2	2	8	-	5	4	1	2	7	8009.2253	0.0004
6	4	2	1	6	-	5	4	1	1	5	8009.3164	-0.0001
6	4	2	2	4	-	5	4	1	2	3	8009.4450	0.0005
5	3	2	2	3	-	4	2	2	2	2	8009.6074	0.0008
5	3	2	2	7	-	4	2	2	2	6	8009.7840	0.0010
5	3	2	1	6	-	4	2	2	1	5	8009.9246	-0.0002
5	3	2	1	4	-	4	2	2	1	3	8010.0128	-0.0004
5	3	2	2	6	-	4	2	2	2	5	8010.0509	0.0006
5	3	2	2	5	-	4	2	2	2	4	8010.1675	-0.0011
6	3	3	2	6	-	5	3	2	2	5	8244.8178	-0.0007
6	3	3	2	7	-	5	3	2	2	6	8245.0580	-0.0001
6	3	3	1	7	-	5	3	2	1	6	8245.1024	-0.0026
6	3	3	2	5	-	5	3	2	2	4	8245.1219	0.0007
6	3	3	2	8	-	5	3	2	2	7	8245.3419	-0.0006
6	3	3	1	6	-	5	3	2	1	5	8245.3631	-0.0020
6	3	3	0	6	-	5	3	2	0	5	8245.3626	-0.0015
6	3	3	2	4	-	5	3	2	2	3	8245.3833	-0.0009
7	3	5	2	7	-	6	3	4	2	6	8856.3484	-0.0006
7	3	5	1	8	-	6	3	4	1	7	8856.4014	0.0017
7	3	5	2	8	-	6	3	4	2	7	8856.4021	0.0013
7	3	5	1	6	-	6	3	4	1	5	8856.4032	0.0001
7	3	5	2	9	-	6	3	4	2	8	8856.4535	0.0006
7	2	5	0	7	-	6	2	4	0	6	9075.1325	-0.0016
7	2	5	2	9	-	6	2	4	2	8	9075.1777	0.0002
7	2	5	2	7	-	6	2	4	2	6	9075.5140	0.0000

<sup>a</sup> The coupling scheme used is:  $I_{Ni} + I_{No} = I_N$ ;  $I_N + J = F$ .

<sup>b</sup> Experimental transition frequency

<sup>c</sup> Experimental transition frequency – theoretical transition frequency

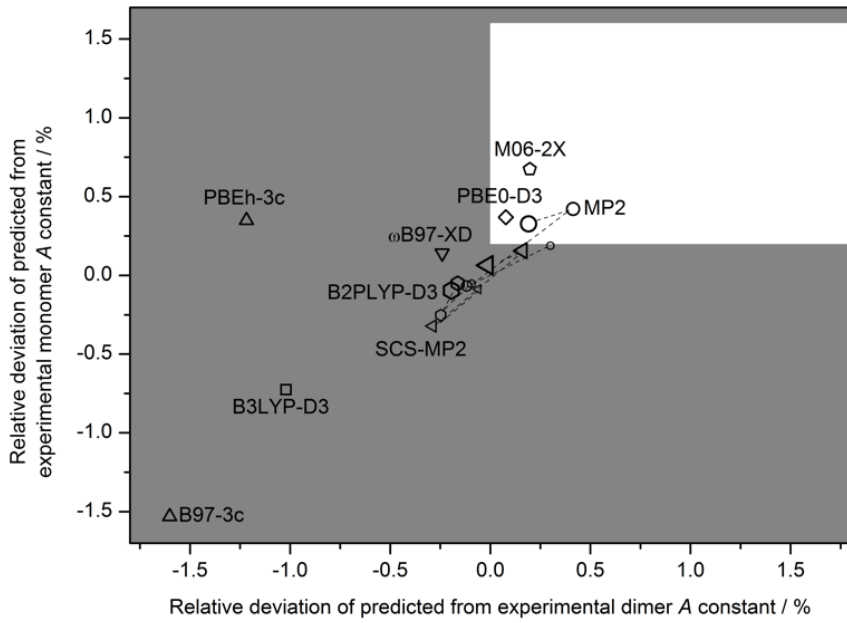


**Figure S2.** Relative deviation of the theoretically predicted ( $A_e$ ) from the experimental rotational constant ( $A_{\text{exp}}$ ) for the HFIP monomer and H<sub>2</sub>NH at different levels of electronic structure calculation. Each method is represented by a symbol. For MP2, SCS-MP2 and B2PLYP-D3, four basis sets (VTZ, aVTZ, VQZ, and aVQZ) were used. Increasing basis set size from VTZ to aVQZ is indicated by progressively larger symbols, which are connected by dashed lines for each method. The zone of estimated incompatibility with experiment is grey. Only predictions within the white area are compatible with experiment for both species, using the lower and upper bounds of vibrational effects on rotational constants, ranging from 0.2% to 1.6% for the HFIP monomer and from 0% to 1.8% for H<sub>2</sub>NH. See the main text for further discussion.

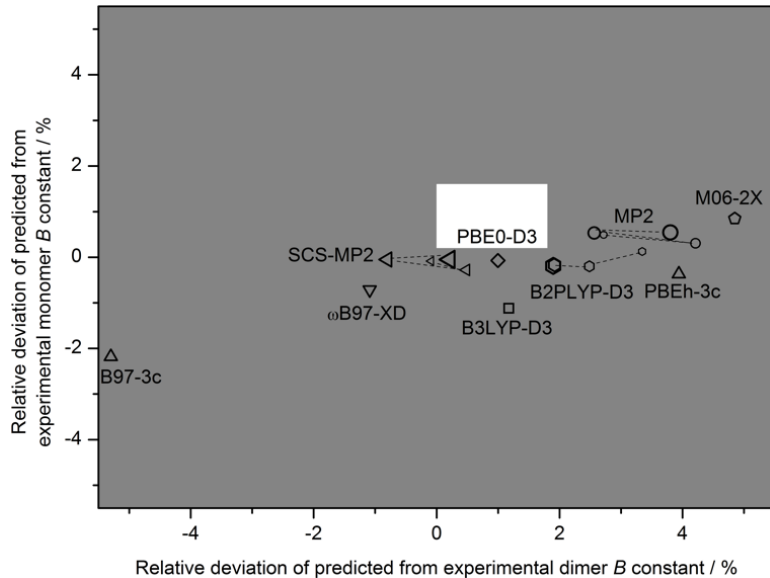


**Figure S3.** Relative deviation of the theoretically predicted ( $B_e$ ) from the experimental rotational constant ( $B_{\text{exp}}$ ) for the HFIP monomer and H<sub>2</sub>NH at different levels of electronic structure calculation. Each method is represented by a symbol. For MP2, SCS-MP2 and B2PLYP-D3, four basis sets (VTZ, aVTZ, VQZ, and aVQZ) were used. Increasing basis set size from VTZ to aVQZ is indicated by progressively larger symbols, which are connected by dashed lines for

each method. The zone of estimated incompatibility with experiment is grey. Only predictions within the white area are compatible with experiment for both species, using the lower and upper bounds of vibrational effects on rotational constants, ranging from 0.2% to 1.6% for the HFIP monomer and from 0% to 1.8% for H<sub>t</sub>N<sub>H</sub>. See the main text for further discussion.

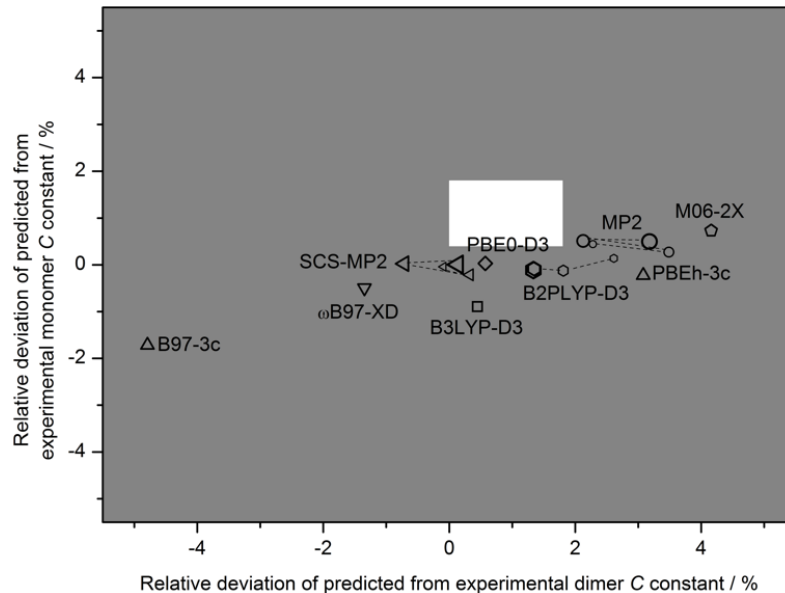


**Figure S4.** Relative deviation of the theoretically predicted ( $C_e$ ) from the experimental rotational constant ( $C_{\text{exp}}$ ) for the HFIP monomer and H<sub>t</sub>N<sub>H</sub> at different levels of electronic structure calculation. Each method is represented by a symbol. For MP2, SCS-MP2 and B2PLYP-D3, four basis sets (VTZ, aVTZ, VQZ, and aVQZ) were used. Increasing basis set size from VTZ to aVQZ is indicated by progressively larger symbols, which are connected by dashed lines for each method. The zone of estimated incompatibility with experiment is grey. Only predictions within the white area are compatible with experiment for both species, using the lower and upper bounds of vibrational effects on rotational constants, ranging from 0.2% to 1.6% for the HFIP monomer and from 0% to 1.8% for H<sub>t</sub>N<sub>H</sub>. See the main text for further discussion.

**Table S5.** Theoretically predicted harmonic ( $\omega_{\text{OH}}$ ) OH stretching wavenumber, hydrogen bond induced downshift ( $\Delta\omega_{\text{OH}}$ ) and lowest predicted wavenumber ( $\omega_1$ , typically CF<sub>3</sub> torsion in H<sub>t</sub> and intermolecular torsion in H<sub>t</sub>N<sub>H</sub>), in cm<sup>-1</sup>, IR intensity ( $S_{\text{OH}}$ ) in km mol<sup>-1</sup>, as well as equilibrium rotational constants ( $A_e$ ,  $B_e$ ,  $C_e$ ) in MHz and magnitudes of the electric dipole moment components ( $|\mu_a|$ ,  $|\mu_b|$ ,  $|\mu_c|$ ) in D calculated at different levels of approximation.

Level of theory	Structure	$\omega_{\text{OH}}$	$S_{\text{OH}}$	$\Delta\omega_{\text{OH}}$	$\omega_1$	$A_e$	$B_e$	$C_e$	$ \mu_a $	$ \mu_b $	$ \mu_c $
B3LYP-D3/	H <sub>t</sub>	3789	63	-	25	2089.8	1042.2	922.9	0.0	0.6	0.1
def2-QZVP	H <sub>t</sub> N <sub>H</sub>	3753	281	36	18	958.2	743.0	535.7	0.8	0.0	0.4
PBEh-3c	H <sub>t</sub>	3895	69	-	34	2112.5	1050.1	930.0	-	-	-
	H <sub>t</sub> N <sub>H</sub>	3883	240	12	20	956.3	763.3	549.7	-	-	-
B2PLYP-D3/ VTZ	H <sub>t</sub> N <sub>H</sub>	3807	65	-	26	2104	1055.3	933.8	-	-	-
B2PLYP-D3/ aVTZ	H <sub>t</sub> N <sub>H</sub>	3778	282	29	21	967.2	758.9	547.2	-	-	-
B2PLYP-D3/ aVQZ	H <sub>t</sub>	3796	66	-	5	2099.8	1051.9	931.0	-	-	-
	H <sub>t</sub> N <sub>H</sub>	3762	273	34	10	965.7	752.6	542.9	-	-	-
B2PLYP-D3/ VQZ	H <sub>t</sub>	3807	70	-	24	2104.1	1052.2	931.5	-	-	-
	H <sub>t</sub> N <sub>H</sub>	3775	280	32	18	966.5	748.4	540.5	-	-	-

B2PLYP-D3/ aVQZ	H <sub>t</sub>	3809	65	-	18	2103.1	1052.0	931.2	-	-	-
	H <sub>t</sub> N <sub>H</sub>	3771	278	38	19	966.2	748.2	540.4	-	-	-
B97-3c	H <sub>t</sub>	3716	43	-	20	2072.9	1031.0	914.2	-	-	-
	H <sub>t</sub> N <sub>H</sub>	3688	189	28	14	952.6	695.4	507.7	-	-	-
M06-2X/ aVTZ	H <sub>t</sub>	3828	82	-	16	2119.3	1062.9	940.0	0.0	0.6	0.1
MP2/ VTZ	H <sub>t</sub>	3818	67	-	28	2109.1	1059.2	937.0	-	-	-
	H <sub>t</sub> N <sub>H</sub>	3787	270	31	13	971	754.3	545.4	-	-	-
MP2/ aVTZ	H <sub>t</sub>	3794	70	-	15	2103.7	1057.2	935.2	-	-	-
	H <sub>t</sub> N <sub>H</sub>	3758	278	36	11	967	765.2	551.9	-	-	-
MP2/ VQZ	H <sub>t</sub>	3819	73	-	25	2114	1059.6	937.7	-	-	-
	H <sub>t</sub> N <sub>H</sub>	3784	275	35	17	972.1	753.1	544.6	-	-	-
MP2/ aVQZ	H <sub>t</sub>	3810	73	-	24	2112	1059.7	937.6	-	-	-
	H <sub>t</sub> N <sub>H</sub>	3772	276	38	15	970	762.2	550.2	-	-	-
PBE0-D3/ aVTZ	H <sub>t</sub>	3830	65	-	24	2112.9	1053.2	932.6	0.0	0.5	0.1
	H <sub>t</sub> N <sub>H</sub>	3786	274	44	18	968.9	741.7	536.3	0.7	0.0	0.3
SCS-MP2/ VTZ	H <sub>t</sub>	3822	62	-	28	2103.3	1053.1	931.9	-	-	-
	H <sub>t</sub> N <sub>H</sub>	3802	232	20	13	967.5	733.7	532.8	-	-	-
SCS-MP2/ aVTZ	H <sub>t</sub>	3801	65	-	16	2098.3	1051.1	930.1	-	-	-
	H <sub>t</sub> N <sub>H</sub>	3778	242	23	13	965.3	737.9	535.0	-	-	-
SCS-MP2/ VQZ	H <sub>t</sub>	3827	67	-	26	2108.4	1053.5	932.6	-	-	-
	H <sub>t</sub> N <sub>H</sub>	3803	237	24	19	969.7	728.4	529.4	-	-	-
	H <sub>t</sub>	3818	68	-	24	2106.5	1053.5	932.4	-	-	-
SCS-MP2/ aVQZ	H <sub>t</sub> N <sub>H</sub>	3792	241	26	14	968	735.9	534.0	-	-	-
ωB97-XD/ aVTZ	H <sub>t</sub>	3860	63	-	21	2108.1	1046.5	927.2	0.0	0.5	0.1
	H <sub>t</sub> N <sub>H</sub>	3816	256	44	17	965.8	726.3	526.1	0.8	0.0	0.3

## References:

- <sup>i</sup> A. Shahi and E. Arunan, *J. Phys. Chem. A*, 2015, **119**, 5650–5657.
- <sup>ii</sup> S. Oswald, N. A. Seifert, F. Bohle, M. Gawrilow, S. Grimme, W. Jäger, Y. Xu and M. A. Suhm, *Angew. Chem. Int. Ed. Engl.*, 2019, **58**, 5080–5084.
- <sup>iii</sup> A. Shahi and E. Arunan, *Phys. Chem. Chem. Phys.*, 2015, **17**, 24774–24782.
- <sup>iv</sup> B. Wu, A. S. Hazrah, N. A. Seifert, S. Oswald, W. Jäger and Y. Xu, *J. Phys. Chem. A*, 2021, **125**, 10401–10409.